Journal of Chromatography B 1265 (2025) 124764

Contents lists available at ScienceDirect

Journal of Chromatography B

journal homepage: www.elsevier.com/locate/jchromb

Targeted mass spectrometry method for the determination of multiple gut-microbiota metabolites in human plasma

Sara R. Fernandes [a,b], Cristian Azorín [c], Eduarda M.P. Silva [d,e], Manuel Miró [f], Luisa Barreiros [a,b,*], Marcela A. Segundo [a,*]

[a] LAQV, REQUIMTE, Department of Chemical Sciences, Faculty of Pharmacy, University of Porto, Rua de Jorge Viterbo Ferreira 228, 4050-313 Porto, Portugal
[b] ESS, Polytechnic of Porto, Rua Dr. António Bernardino de Almeida 400, 4200-072 Porto, Portugal
[c] GICAPC Research Group, Department of Analytical Chemistry, University of Valencia, Calle Dr. Moliner 50, 46100 Burjassot, Valencia, Spain
[d] Associate Laboratory i4HB - Institute for Health and Bioeconomy, University Institute of Health Sciences - CESPU, 4585-116 Gandra, Portugal
[e] UCIBIO - Applied Molecular Biosciences Unit, University Institute of Health Sciences - CESPU (1H-TOXRUN, IUCS-CESPU), 4585-116 Gandra, Portugal
[f] FI-TRACE group, Department of Chemistry, University of the Balearic Islands, Carretera de Valldemossa km 7.5, E-07122 Palma de Mallorca, Spain

ARTICLE INFO

Keywords:
Gut metabolites
Chemical derivatization
Targeted analysis
Mass spectrometry
Biomatrices
Clinical diagnostics

ABSTRACT

The gut microbiota profoundly impacts human health by producing metabolites that can act as biomarkers for disease diagnosis and therapy. However, accurately measuring these metabolites in biomatrices is challenging due to their low concentrations, high molecular diversity, and interference from matrix components, demanding advanced and precise analytical methodologies. Hence, an ultra-high-performance liquid chromatography method coupled to triple quadrupole-tandem mass spectrometry detection, combined with a chemical derivatization procedure, was developed and validated to quantify seven gut metabolites, namely acetic acid, propionic acid, butyric acid, *p*-cresol sulfate, 3-indoxyl sulfate, indole-3-acetic acid, and L-tryptophan, in human plasma. Samples were prepared by protein precipitation with acetonitrile and subsequently derivatized using 3-nitrophenylhydrazine. Chromatographic separation was achieved using a BEH C18 column, with elution performed at a flow rate of 0.2 mL min^{-1} and in gradient mode using formic acid-water (1:1000, *v/v*) and formic acid-acetonitrile (1:1000, *v/v*) as mobile phase components. The mass spectrometer was operated in negative ionization mode and data was acquired in selected reaction monitoring. Good linearity was achieved ($r^2 > 0.997$) for all the target gut metabolites in the evaluated concentration ranges, with low LLOQ values (0.4–8 μM). The method proved to be accurate (87.0–114 %) and precise (CV ≤ 13.5 %), achieving a score of 65 in the Blue Applicability Grade Index (BAGI) metric, which confirmed its practicality. The developed method was ultimately employed to the analysis of plasma samples from children and adults involved in clinical studies, demonstrating its usefulness in medical research.

1. Introduction

The gut microbiome is a complex and dynamic ecosystem that plays a critical role in human health and disease [1–3]. Understanding the mechanisms underlying the gut-host interactions requires a comprehensive analysis of the gut-derived metabolites, which are produced by microorganisms or originated from modifications of host or external molecules, and can act as biomarkers of the host's status [4,5]. Despite recent advances in analytical methods, the measurement of gut metabolites in biological fluids is still challenging, due to their low concentrations and high molecular diversity [3,6,7]. Short-chain fatty acids (SCFAs) and amino acids (e.g. tryptophan (TRP)) and their derivatives (such as TRP and tyrosine (TYR) derivatives) are the classes of gut metabolites that have received most attention over the years due to their role as endogenous biomarkers of the development and progression of chronic diseases [1–3,5,8,9].

SCFAs are a class of carboxylic acids with a short 2–6 carbon alkyl chain, produced by microbial fermentation of non-digestible dietary fibers and through the degradation of proteins and amino acids [1,2,8,10,11]. The most abundant SCFAs in humans are acetic acid (AA), propionic acid (PA), and butyric acid (BA), which together account for ≥95 % of all SCFAs produced in the gut [2,5,8]. These are important

* Corresponding authors: LAQV, REQUIMTE, Departamento de Ciências Químicas, Faculdade de Farmácia, Universidade do Porto, Rua de Jorge Viterbo Ferreira 228, 4050-313 Porto, Portugal.
E-mail addresses: lbarreiros@ff.up.pt (L. Barreiros), msegundo@ff.up.pt (M.A. Segundo).

https://doi.org/10.1016/j.jchromb.2025.124764
Received 23 April 2025; Received in revised form 30 July 2025; Accepted 10 August 2025
Available online 14 August 2025

metabolites that play multiple functions, namely energy source, gut integrity, metabolism and immune system regulation, anti-inflammatory and antitumorigenic activity, among others [1,3,10,12].

TRP is an essential amino acid that must be obtained through dietary sources [2,5]. TRP is used by the body to synthesize proteins and is also a precursor for several important bioactive metabolites that play key roles in the organism, including protein synthesis, neurotransmitter synthesis (e.g., serotonin), hormonal regulation, and immune function [2,4,13]. TRP can be metabolized by several pathways in the body, namely the kynurenine pathway, the serotonin pathway, and the indole pathway [2–5].

Through the indole pathway, TRP can be directly converted by intestinal microbiome to indole and its derivatives, such as indoxyl sulfate (INDS) and indole-3-acetic acid (IAA) [3]. These two compounds and *p*-cresol sulfate (pCS), that is a derivative of the amino acid TYR, are also gut-derived metabolites that play an important role in the host status. Indeed, these metabolites are small molecules that have a low renal clearance and can accumulate in the organism due to their high affinity for plasmatic proteins [14,15]. Therefore, an association has been demonstrated between their plasmatic levels and renal failure, as well as the progression of chronic kidney disease (CKD) [14,16,17].

Different analytical approaches have been developed for the determination of the mentioned classes of gut metabolites in biomatrices. Regarding SCFAs, their determination in biological samples (e.g., blood, serum, plasma, feces) has been generally performed using gas chromatography (GC) coupled with flame ionization detector (FID) or mass spectrometry (MS) detectors [3,18], due to their volatility. Additionally, alternative methodologies based on liquid chromatography (LC) and capillary electrophoresis (CE) coupled with MS detection have been developed more recently to improve the limits of detection and quantification achieved with the GC–MS technique [3,12,18,19]. Despite the advantages associated to LC-MS techniques, the direct analysis of SCFAs by LC-ESI-MS is challenging, due to the poor ionization and retention in reversed-phase chromatography, high volatility, high polarity, and low molecular weight of these compounds [3,12,18,19]. Hence, chemical derivatization procedures using different reagents (e.g., 3-nitrophenylhydrazine (3-NPH), *O*-benzylhydroxylamine (O-BHA), aniline and Girard's reagent T) have been developed to overcome some of the difficulties associated with their determination by LC-MS [3,12,18–21]. The implementation of such procedures improves the analytical performance through the increase of the molecular size and the hydrophobicity of SCFAs that favors retention in reversed-phase LC systems and leads to a higher sensitivity and selectivity of MS detection [3,12,18–21]. In the case of TRP and TYR derivatives, LC-MS methods are the most commonly applied methodologies for their quantification in different biomatrices, without the need of implementing additional procedures before analysis to improve the analytical performance as referred for SCFAs [3,19,22,23]. Nevertheless, some methodologies determining simultaneously SCFAs and other gut-derived metabolites (e.g., IAA and TRP) implemented chemical derivatization to achieve their concomitant determination [19,24].

Considering the recognized relevance of gut metabolites in the transition between health and disease, the establishment of analytical methods that allow the simultaneous measurement of their circulating levels in blood is of utmost importance. In fact, a snapshot of the host's status can be obtained through the assessment of the circulating levels of these compounds in the body. Consequently, a fast diagnosis and the definition of the best treatment strategy can be pursued, namely for metabolic diseases (e.g., obesity and diabetes), cardiovascular diseases (e.g., atherosclerosis and ischemic heart), gastrointestinal diseases (e.g., Crohn's disease and inflammatory bowel disease), neurological and psychiatric disorders (e.g., Alzheimer's disease and depression), and cancer [2,25,26]. Additionally, these methods can shed light on current challenges concerning the role of gut microbiota in different parts of the body, for example the gut-brain axis [27,28]. It should be noted that the chromatographic methods previously described in the literature only focused on the determination of SCFAs or SCFAs combined with TRP and IAA, with no inclusion of the other indole products (e.g., INDS) and derivatives from other amino acids (pCS) [19,24,29–31]. Hence, the main goal of the present work was the development of an ultra-high-performance liquid chromatography method coupled to triple quadrupole-tandem mass spectrometry detection (UHPLC-MS/MS) for the simultaneous determination of seven gut metabolites in human plasma samples after a rapid and simple protein precipitation procedure combined with a chemical derivatization step, using 3-NPH as derivatization reagent.

2. Materials and methods

2.1. Chemicals, reagents, and solutions

Ultra-pure water (resistivity >18 MΩ cm) used for the preparation of all the solutions was obtained from an Easy 15 water purification system (Heal Force, Shanghai, China). Acetic acid (AA), [$^2H_4$]-acetic acid (AA-IS), propionic acid (PA), butyric acid (BA), 3-indoxyl sulfate potassium salt (INDS), indole-3-acetic acid sodium salt (IAA), and L-tryptophan (TRP) were purchased from Merck KGaA (Darmstadt, Germany). *p*-Cresol sulfate ammonium salt (pCS), [$^2H_4$]-*p*-cresol sulfate ammonium salt (pCS-IS), [$^2H_6$]-propionic acid (PA-IS), and [$^2H_5$]-kynurenic acid (KYNA-IS) were obtained from Alsachim (Illkirch Graffenstaden, France). [$^2H_4$]-3-Indoxyl sulfate (INDS-IS) was acquired from Toronto Research Chemicals Inc. (Toronto, Canada), through LGC standards. Acetonitrile (ACN, LiChrosolv LC-MS grade), dimethyl sulfoxide (DMSO), and formic acid were purchased from Merck KGaA. The derivatization reagents, 3-nitrophenylhydrazine hydrochloride (3-NPH), *N*-(3-dimethylaminopropyl)-*N*-ethylcarbodiimide hydrochloride (EDC) and pyridine (anhydrous, 99.8 %), were also purchased from Merck KGaA.

Stock solutions of all the target analytes and the internal standards (IS) (Fig. S1) were prepared separately at different concentrations in water, ACN, a mixture of ACN and H_2O (50:50, *v/v*), or DMSO (Table S1), according to their solubility, and stored at −20 °C. A working solution was prepared in water by mixing all the target analytes to final concentrations of 10 μM for IAA, 25 μM for PA and BA, 100 μM for INDS and TRP, 150 μM for AA, and 200 μM for pCS. Subsequently, this working solution was used for preparing the calibration standards (Table S2), by dilution in water, and the quality control (QC) samples. A similar working solution of internal standards was prepared by mixing all the IS to concentrations of 100 μM for pCS-IS, 125 μM for KYNA-IS, 250 μM for PA-IS and INDS-IS, and 500 μM for AA-IS, yielding final concentrations in the extract of 10 μM for pCS-IS, 12.5 μM for KYNA-IS, 25 μM for PA-IS and INDS-IS, and 50 μM for AA-IS.

Regarding derivatization solutions, they were prepared daily in a mixture of ACN and water (50:50, *v*/v) at concentrations of 200 mM for 3-NPH, 120 mM for EDC, and 6 % (*v/v*) for pyridine. A mixture of the three reagents solutions was prepared in a proportion of 1:1:1 (*v/v/v*) and used for the derivatization procedure.

2.2. Sample preparation and derivatization procedure

To precipitate proteins, an aliquot of 100 μL of human plasma was mixed with 10 μL of IS working solution, followed by 290 μL of ACN. The mixture was vortexed for 1 min, and subsequently centrifuged at 12,100 ×*g* for 10 min at 4 °C. The resulting supernatant was collected and submitted to the derivatization procedure. The calibration standards, a zero sample prepared in water (spiked only with IS), and the QC samples, prepared both in water and in pooled human plasma, were treated under the same conditions.

For the derivatization procedure, 150 μL of the mixture of derivatization reagents (200 mM of 3-NPH, 120 mM of EDC, and 6 % (*v*/v) of pyridine) were added to 100 μL of the supernatant obtained after protein precipitation. This mixture was then allowed to react at 25 °C in an

Eppendorf ThermoMixer® C (Hamburg, Germany) for 30 min, protected from light with aluminium foil. Afterwards, the derivatized extract was placed in ice for 2 min, subsequently diluted 2× in water and centrifuged at 12,100 ×*g* for 5 min, at room temperature. Finally, the supernatant was transferred into a vial, and a volume of 4 µL was injected into the UHPLC-MS/MS system for analysis.

2.3. UHPLC-MS/MS conditions

2.3.1. Instrumentation

A Nexera X2 Ultra High-Performance Liquid Chromatograph (UHPLC) system (Shimadzu Corporation, Kyoto, Japan), equipped with two LC-30AD pumps, a DGU-20A5R degassing unit, an SIL-30AC autosampler and a CTO-20AC oven, coupled with a LCMS-8040 triple quadrupole mass spectrometer (Shimadzu Corporation) with an electrospray ionization source (ESI), was used to perform the LC-MS/MS analysis. The instrument control, all chromatographic data acquisition and processing were performed using the LabSolutions software version 5.60 SP2 (Shimadzu Corporation).

2.3.2. Chromatographic and mass spectrometric conditions

The chromatographic separation was carried out on a BEH C18 column (2.1 × 100 mm, 1.7 µm particle size) from Waters® (Milford, USA), using formic acid-water (1:1000, *v/v*) (solvent A) and formic acid-ACN (1:1000, *v/v*) (solvent B) as mobile phase components. The separation was achieved by a gradient elution at a flow rate of 0.2 mL min^{-1}. The LC gradient applied was as follows: 0–0.5 min,15 % B; 0.5–12.5 min, 15–55 % B; 12.5–13.5 min, 55–100 % B; 13.5–15.5 min, 100 % B; 15.5–16.5 min, 100–15 % B; and 16.5–18.5 min, 15 % B. The autosampler was kept at 6 °C, and the column oven was set to 40 °C during the analysis.

The MS was operated in negative electrospray ionization mode (ESI-), and the source parameters were as follows: nebulizing gas (N_2) flow rate at 2.9 L min^{-1}, drying gas (N_2) flow rate at 15.0 L min^{-1}, desolvation line temperature at 300 °C, heat block temperature at 425 °C, detector voltage at 2.02 kV, collision gas (argon) at 230 kPa. Data was acquired in selected reaction monitoring (SRM) mode. The SRM transitions for all the analytes and internal standards are presented in Table 1, as well as the retention time values, and some optimized MS operating parameters (collision energies, and Q1 and Q3 Pre-Bias voltage).

2.3.3. Method validation

The proposed methodology was validated for linearity and dynamic range, intra- and inter-day accuracy and precision, lower limit of quantification (LLOQ), and carry-over effects according to European Medicines Agency (EMA) and International Council for Harmonisation of Technical Requirements for Pharmaceuticals for Human Use (ICH) guideline [32]. Moreover, the stability of the derivatized analytes stored at the autosampler was assessed.

The linearity and working range were assessed by the analysis of standards, prepared and acquired in triplicate, in three independent runs, covering the expected physiological concentrations of these metabolites in serum/plasma within the following ranges: 6–150 µM for AA; 1–25 µM for PA and BA; 8–200 µM for pCS; 4–100 µM for INDS and TRP; and 0.4–10 µM for IAA (Table S2). The calibration curves were constructed by plotting the peak area ratio of each analyte with its corresponding IS (Analyte/IS, Table S1) versus analyte nominal concentration of seven standard solutions of each target analyte prepared in water. Back-calculated concentrations of the calibration standards were also determined as recommended by the guidelines [32]. Additionally, a zero sample (only with IS), prepared in water, was included in each analytical run. The LLOQ was defined as the lowest calibration standard concentration.

Accuracy and precision (intra- and inter-day) were determined by assaying QC samples prepared in water and in plasma at four concentration levels (6, 15, 60, and 120 µM for AA; 1, 2.5, 10 and 20 µM for PA and BA; 8, 20, 80, and 160 µM for pCS; 4, 10, 40, and 80 µM for INDS and TRP; and 0.4, 1, 4 and 8 µM for IAA). Because the target analytes are endogenous compounds of plasma, a zero QC sample (plasma spiked only with the IS, i.e., similar to the zero sample) was also prepared and analyzed under the same conditions. Accuracy was calculated as the percentage of the found concentrations versus nominal concentrations, while precision was expressed as the coefficient of variation (CV). To assess intra-day precision and accuracy, data from three consecutive injections ($n = 3$) of each QC aqueous standard or six consecutive injections ($n = 6$) of each QC prepared in plasma were used, followed by interpolation of the values in the calibration curve. Inter-day values

Table 1
Selected reaction monitoring (SRM) conditions and retention times for the determination of the target analytes and internal standards in plasma samples.

Compound	Precursor ion (*m/z*)	Product ions[a] (*m/z*)	Q1 Pre-Bias (V)	Collision energy (eV)	Q3 Pre-Bias (V)	Retention time (min)
Acetic acid (AA)	193.90	**152.00**[b]	12	15	30	5.22
		137.00	12	20	25	
Propionic acid (PA)	207.90	**137.05**[b]	13	20	25	6.16
		164.85	13	13	15	
Butyric acid (BA)	222.00	**152.05**[b]	14	14	30	7.80
		179.10	14	11	19	
p-Cresol sulfate (pCS)	187.00	**107.05**	12	17	30	4.78
		79.95	12	20	20	
3-Indoxyl sulfate (INDS)	212.00	**80.05**	14	23	30	3.92
		132.05	14	18	25	
Indole-3-acetic acid (IAA)	309.00	**137.05**[b]	21	22	26	10.06
		116.10	21	20	21	
L-Tryptophan (TRP)	338.00	**136.95**[b]	23	25	26	5.99
		209.15	22	19	14	
[$^2H_4$]-Acetic acid	196.90	**137.10**[b]	12	20	25	5.19
		46.10	12	35	18	
[$^2H_6$] – Propionic acid	212.90	**137.05**[b]	13	17	26	6.10
		170.10	13	10	18	
[$^2H_4$] - *p*-Cresol sulfate	190.90	**111.05**	12	20	21	4.77
		80.05	12	17	15	
[$^2H_4$] - 3-Indoxyl sulfate	215.90	**80.05**	14	21	30	3.82
		136.10	14	17	25	
[$^2H_5$] – Kynurenic acid	327.80	**147.10**[b]	21	25	27	7.82
		150.05	21	22	29	

[a] Ions selected for quantitative analysis written in bold. [b] Ions originated by the derivatized target compound.

were calculated using data from three independent experiments ($n = 3$).

The potential for carry-over was evaluated by injecting ACN-H_2O (50:50, *v/v*) immediately after analyzing the highest calibration standard and after completing the analysis of five consecutive samples.

The stability of the derivatized analytes was assayed by analysis of QC samples prepared in water and in plasma, which were stored in the autosampler of the LC-MS instrument, at 6 °C, for 24 and 48 h. The stability was assessed at one concentration level: 15 μM AA; 2.5 μM PA and BA; 20 μM pCS; 10 μM INDS and TRP; and 1 μM IAA for water; 30 μM AA; 5 μM PA and BA; 40 μM pCS; 20 μM INDS and TRP; and 2 μM IAA for plasma. The concentration of each analyte after the storage period was compared to the nominal concentration.

2.3.4. Application to clinical samples

The developed method was applied to plasma samples from five children (aged between 5 and 10 years old) participating in the M2Child study and five adults (aged between 18 and 65 years old) participating in the Microbi-A study. The M2Child study had the main goal of exploring the microbiota-gut-brain axis in Attention Deficit Hyperactivity Disorder (ADHD). Besides children with ADHD disorder, healthy children were included as controls in this study. On the other hand, the Microbi-A study involved adult participants and aimed at evaluating the relationship between the human microbiome and personality traits. The adults were all healthy individuals. Overall, the samples analyzed in the present work included 3 healthy children, 2 children with ADHD and 5 healthy adults.

The study protocols for M2Child and Microbi-A were approved by the Ethics Committee for Health of *Centro Hospitalar Universitário de São João* (approval number 318/2020) and the Ethics Committee for Health of *Faculdade de Psicologia e de Ciências da Educação da Universidade do Porto* (approval number 2020/12-01b), respectively, and followed the 1964 Helsinki declaration and its later amendments. All participants were volunteers and written informed consent was obtained from the participant or from the legal guardian (in the case of children). Blood was collected by trained nurses and immediately centrifuged at 5000 rpm (3892 ×*g*) for 15 min at 4 °C for plasma separation. Plasma was immediately frozen and stored at −80 °C until analysis. After thawing, samples were treated as described in *section 2.2. Sample preparation and derivatization procedure* and analyzed by the developed UHPLC-MS/MS method.

3. Results and discussion

3.1. Development of the UHPLC-MS/MS method

The seven target gut metabolites present different physicochemical properties, namely hydrophobicity, but all are moderately polar (log *P* values between −1.09 (TRP) and 1.71 (IAA), Table S3). On the other hand, the implemented derivatization procedure leads to chemical structure modifications by introducing specific functional groups [33,34]. Consequently, the physicochemical properties of the analytes are affected, namely solubility, polarity, stability, reactivity, and volatility [33,34]. Regarding the target analytes, it is important to consider that most of them were derivatized (AA, PA, BA, IAA, TRP) by reaction with 3-NPH, but two of them (pCS and INDS) did not react, as expected, with the derivatizing reagent and maintained the original properties after the derivatization procedure (Fig. S1). One of the main changes induced by the chemical derivatization procedure was the polarity of the analytes. In fact, a decrease in polarity was observed for all the derivatized compounds shown by the increment of log *P* (values between 1.01 (AA) and 2.9 (IAA), Table S3), which were considered for the selection of the chromatographic conditions (stationary phase, and mobile phase composition), and for definition of the MS/MS detection parameters for the derivatized compounds.

3.1.1. Study of MS detection conditions and fragmentation pathways

MS/MS applications are of crucial importance in the clinical field for high selectivity and sensitivity analysis [35–37], but also for structure characterization and elucidation of fragmentation mechanisms [38,39]. In this study, the determination of the optimal SRM transitions for each gut metabolite was conducted using the scan mode by flow injection analysis-ESI-MS/MS at a flow rate of 0.2 mL min^{-1}. The negative ionization mode was selected over the positive one since the hydrogens in the hydrazine moiety of the 3-NPH derivatized compounds are easily lost, because of their acidic character enhanced by the strong electron-withdrawing nature of the nitro group (-NO_2) on the phenyl ring. Moreover, the anionic species formed can be stabilized by electron delocalization across the aromatic system, increasing the stability of the resulting anion, and further increasing the ionization efficiency in the negative mode. Since pCS and INDS have low pKa (−2.04 and −1.82), they are fully deprotonated under physiological pH, not necessarily requiring derivatization with 3-NPH for analysis under ESI-. Hence, the negative pseudo-molecular ions $[M\text{-}H]^-$ were obtained in the Q1 spectrum of all analytes (Fig. S2-S9) and were chosen to obtain the product ion spectra. The fragmentation patterns and formed product ions, in each case, were examined to analyze and characterize the product ion chosen for the quantification and to proceed with the selection of the identification ion (Table 1, Fig. S2-S9). The highest intensity ion was selected for quantification to maximize sensitivity and improve the limits of detection, whereas the second most intense ion was selected for identity confirmation.

Fragmentation of the 3-NPH-derivatized carboxylates, namely AA-3NPH, PA-3NPH, BA-3NPH, and IAA-3NPH is characterized by the formation of the 3-nitroaniline anion at *m/z* 137 (product ion **3**, Fig. S2-S4 and S7). Considering, e.g., compound AA-3NPH, this product ion **3** is possibly formed by an initial [1,3]-hydrogen shift from the α carbon to the nitrogen atom leading to the formation of an enolate (Fig. S2B, structure **2**) and subsequent loss of an aziridinone molecule through enolate rearrangement. The product ion at *m/z* 152 (Fig. S2, S4 and S7) is, likewise, a characteristic product ion which is formed through a [1,3]-hydrogen shift, cleavage of the carbonyl-nitrogen bond and formation of a diazobicyclo derivative that allows, as mentioned previously, negative charge stabilization due to the presence of the strongly electron-withdrawing nitro group (Fig. S2B, structure **1**) [40]. The product ion observed at *m/z* 46 used for, e.g., AA-3NPH-IS (Fig. S2) as an identification ion could be explained by the formation of nitrite (NO_2^-), a characteristic fragmentation of nitro-substituted compounds that has been previously described for aromatic nitro-compounds [41]. The neutral loss of 43 Da is also common to several of the studied 3-NPH-derivatized carboxylates, namely PA-3NPH (Fig. S3) and BA-3NPH (Fig. S4). In the case of PA-3NPH, for example, this fragmentation can be explained by the elimination of isocyanic acid (HNCO) from product ion **7**, leading to the product ion at *m/z* 165 (Fig. S3, structure **8**). Confident identification and confirmation of the postulated fragmentation pathways were achieved by studying the fragmentation data analysis of isotopically labeled standards, [$^2H_4$]-AA-3NPH and [$^2H_6$]-PA-3NPH, that delivered identical and corresponding product ions (Fig. S2 and S3).

The sulfate metabolites pCS and INDS were monitored by the formation of the product ions at *m/z* 107 and 132, respectively (Fig. S5 and S6, structures **11** and **14**, respectively), consistent with the neutral loss of 80 Da, and confirming the presence of the sulfate group (-SO_3) in these molecules. The formation of the product ion at *m/z* 80 for both molecules also offers confirmation of the sulfate group [42–44]. The same fragmentation pattern is observed for the corresponding deuterated counterparts ([$^2H_4$]-pCS and [$^2H_4$]-INDS) employed as internal standards, confirming the postulated fragmentation pathways for MS/MS transitions used for quantification and identity confirmation of these compounds (Fig. S5 and S6).

Concerning the derivatized indole metabolites, IAA-3NPH and L-TRP-3NPH (Fig. S7 and S8), the product ion **3** is also observed at *m/z*

137 for both compounds and was selected as quantifying SRM transition. As qualifying ion for compound IAA-3NPH, the indole anion at *m/z* 116 formed by neutral loss of 193 Da (Fig. S7, structure **17**) was chosen. For L-TRP-3NPH, the product ion **22** (Fig. S8) was considered for identity confirmation. The aminoethenolate, observed at *m/z* 209, is probably obtained after a [1,3] proton transfer leading to structure **21** with the subsequent loss of the indole stabilized carbene **23**, as depicted in Fig. S8B.

The postulated fragmentation pathways described for the KYNA-3NPH internal standard (Fig. S9) consider both heterolytic and homolytic cleavages under collision-induced dissociation (CID) conditions. The fragmentation of deprotonated molecules $[M-H]^-$ generally complies with the even-electron rule, meaning that the product ions formed by loss of neutral molecules result in even-electron ions [39,41,45]. This is the case of the mechanisms suggested for the formation of product ions at *m/z* 150 and 122 (Fig. S9, structures **30**/**32** and **31**, respectively). For the product ion at *m/z* 150, two different pathways are proposed considering the deprotonation of the hydrazine moiety in both nitrogen atoms (structures **26** and **27**) resulting from proton transfer of the initially formed $[M-H]^-$. The mechanism devised for structure **27** also justifies the formation of the product ion at *m/z* 178, the 3-nitrophenyl isocyanate **29**. Both proposed mechanisms provide the formation of product ion **31** by losses of neutral molecules N_2 or CO. Even-electron ions produced under ESI conditions can also yield odd-electron ions by homolytic cleavage under CID conditions [39,41,45]. The proposed mechanism for product ions at *m/z* 151 and 147 (Fig. S9B) encompasses homolytic cleavage leading to distonic hypervalent radical anions **33** and **34** at *m/z* 151 and 147, respectively. It is important to refer that these are putative fragmentation mechanisms and confirmation of the proposed pathways could be achieved by HRMS. Nevertheless, a previous work considering the gas-phase structural characterization of neuropeptides Y Y1 receptor antagonists demonstrated that experiments acquired in QqQ showed a good agreement with those obtained in an Orbitrap instrument [38].

3.1.2. Selection of chromatographic conditions

Despite the large number of stationary phase chemistries that have been previously applied for the separation of the target gut metabolites, reversed-phase C18 columns were the most frequently employed in combination with gradient elution profiles using mobile phases containing polar (e.g., water) and organic modifiers (e.g., ACN) acidified with formic acid (e.g., 0.1 %) [3,12,22,46]. Considering this, the separation was evaluated in this work using a BEH C18 column and using formic acid-water (1:1000, *v/v*) and formic acid-acetonitrile (1:1000, *v/v*) as mobile phase components. Furthermore, gradient elution was employed to achieve an efficient separation of the different analytes, considering also possible matrix interfering species.

To attain separation in a short period of time, a study of the elution conditions was performed, which evaluated the influence of gradient starting time and the percentage of organic solvent at the beginning of the gradient. Two different gradient starting time values were tested, namely 5 and 0.5 min (elution conditions 1 (EL1) and elution conditions 2 (EL2), respectively), with 5 % (*v/v*) of organic content (solvent B) at the beginning of the gradient. The obtained results (Fig. 1) show that this parameter had no influence on the separation of most compounds, except for PA and TRP, which partially overlapped (Table 1). Moreover, a decrease in the retention time of all target analytes was observed in EL2. Subsequently, a study of the initial percentage of organic solvent at the beginning of the gradient was performed, starting the gradient at 0.5 min, and using 5, 10, and 15 % of ACN, corresponding to elution conditions 2 (EL2), 3 (EL3), and 4 (EL4). As depicted in Fig. 1, the content of organic solvent at the beginning of the gradient only reduced the retention time of all target analytes but had no effect in their separation. The close elution of PA and TRP with EL2, EL3 and EL4 conditions did not affect their accurate determination due to the use of separate channels for the selected monitoring of each compound. Hence, an

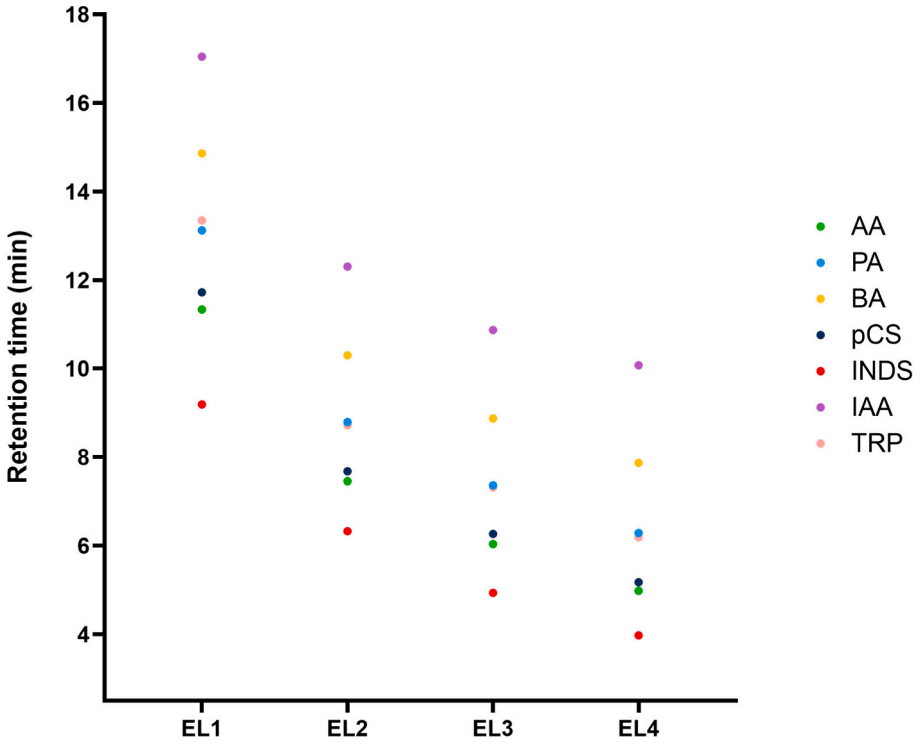

Fig. 1. Effect of the different elution programs tested on the retention time of target analytes. Results obtained from the analysis of a derivatized standard solution prepared in water containing 100 μM of pCS, INDS and IAA, 500 μM of AA, PA, and BA, and 1000 μM of TRP. Mobile phase components: formic acid-water (1:1000, *v/v*) (solvent A) and formic acid-ACN (1:1000, v/v) (solvent B). EL1 (elution conditions 1): gradient starting time at 5 min with 5 % (*v/v*) of solvent B; EL2 (elution conditions 2): gradient starting time at 0.5 min with 5 % (v/v) of solvent B; EL3 (elution conditions 3): gradient starting time at 0.5 min with 10 % (v/v) of solvent B; EL4 (elution conditions 4): gradient starting time at 0.5 min run with 15 % (v/v) of solvent B.

elution program that starts with 15 % (*v/v*) of ACN during 0.5 min (EL4) and increases up to 55 % (*v/v*) in 12 min, at a flow rate of 0.2 mL min^{-1}, was selected as the elution program to achieve efficient separation of all the compounds in a suitable analysis time (18.5 min).

Considering the polarity of the target analytes after the chemical derivatization procedure, the expected elution order of the analytes was AA, INDS, pCS, PA, BA, TRP and IAA (Table S3). However, as can be seen in Fig. 1, the elution profile obtained with the selected chromatographic conditions (EL4) presented differences in the elution order of the compounds, namely INDS that eluted first than AA, and TRP that eluted before PA and BA. These differences allowed to conclude that not only the polarity of the compounds may have affected the elution of the target analytes, but also other factors may have contributed to the results, such as solubility and reactivity (type of interactions established between the analytes and the stationary phase). The most evident example was TRP, which presented a lower polarity (log $P = 2.4$) compared to PA (log $P = 1.7$) and BA (log $P = 2.2$) but eluted first. IAA was the only compound that eluted from the reversed-phase column according to its polarity and, independently of the chemical derivatization, it was always the last compound to be eluted (Table S3).

3.2. Establishment of the derivatization conditions

A chemical derivatization procedure was implemented in the present work to allow the simultaneous quantitation of the three groups of gut metabolites in a single LC-MS/MS run. The use of 3-NPH has been reported previously for the determination of SCFAs and TRP metabolites in biological samples in combination with other reagents (namely, EDC as a coupling reagent and pyridine as a catalyst and base), with significant improvements in the detection limit and chromatographic behavior of these analytes [19,24]. As referred before, other derivatization reagents, such as aniline, *O*-benzylhydroxylamine (O-BHA), and Girard's reagent T (GT), have been used for the derivatization of different classes of gut metabolites. Nevertheless, the efficacy of these methods varies considerably, particularly in the context of SCFA analysis, when compared to 3-NPH. Aniline reacts with carboxylic acids to form amide derivatives when it is combined with EDC or other similar coupling agent [21,47]. Studies comparing the derivatization efficiency of aniline with 3-NPH showed that it is less efficient [47–49]. Indeed, derivatization efficiencies ranging from 20 to 100 % can be attained for aniline derivatives, and high yield variations can be observed between reactions in solvents and real matrices, which makes this reagent unsuitable for the derivatization of SCFAs in complex matrices, such as plasma [47–49]. GT reagent introduces a permanent positive charge (quaternary ammonium group) to the molecule, significantly improving ionization efficiency [18,20]. A recent study that applied this reagent and compared its efficiency with 3-NPH revealed that the sensitivity of GT-derivatives can been approximately 100 times higher, making this reagent an appropriate choice for these metabolites particularly when positive ionization mode is implemented [18,20]. However, GT is less commonly used for SCFAs than 3-NPH and standard protocols are lacking or require careful optimization to achieve complete derivatization and to prevent potential side reactions [18,20]. In contrast to GT, O-BHA is one of the most frequently employed derivatization agents for SCFAs derivatization, along with 3-NPH and, generally, O-BHA derivatives exhibit higher sensitivity in mass spectrometry analysis [18,21,50]. However, compared to 3-NPH, O-BHA requires a longer reaction time and has a higher toxicity profile, making 3-NPH a safer alternative [18,21,50]. Taking all of this into account, a chemical derivatization reaction using 3-NPH in combination with EDC and pyridine was selected over the other mentioned reagents (Fig. S10).

To establish the derivatization conditions for the seven analytes, different parameters that may affect the efficiency of the derivatization reaction were evaluated, such as reagents concentration, the influence of pyridine in the reaction yield, and the time and the temperature of the reaction.

The effect of reagents concentration and the effect of reaction time were evaluated simultaneously using individual standards of SCFAs, since they are the compounds most affected by the derivatization. Three different concentrations of 3-NPH (200, 100 and 50 mM) and EDC (120, 60 and 50 mM), and three reaction times (10, 30 and 60 min) were evaluated, using 6 % (*v/v*) of pyridine, at 25 °C. As shown in Fig. 2, higher signal intensities of all SCFA derivatives were observed for lower concentrations of 3-NPH (100 and 50 mM) and EDC (60 and 50 mM). Nevertheless, even after 60 min of reaction, the signal intensity for all the SCFAs derivatives continued to increase when these derivatization conditions were used. Contrary to this, for higher concentrations of both reagents (200 mM 3-NPH and 120 mM EDC), the signal intensity of the derivatives was slightly lower compared to the previous conditions, but the values were stable after 30 min of reaction (Fig. 2). Hence, these last conditions and a reaction time of 30 min were chosen to perform the next experiments, towards a faster analytical procedure and a better method robustness. Moreover, considering the possibility of using an equipment that allows processing and incubating simultaneously multiple samples (up to 24), the derivatization throughput might be further enhanced.

Pyridine is a common reagent used as a catalyst and base in the derivatization reaction of SCFAs. Despite this, some works referred that the use of pyridine should be avoided to circumvent the possible appearance of interferences, namely the background noise that affects the determination of AA [11,19]. Thus, the possible interference of pyridine in the derivatization reaction efficiency was evaluated. For this study, standards containing only SCFAs, and standards prepared with all the target analytes were derivatized during 30 min using the selected concentrations of 3-NPH and EDC, without or with 6 % (*v/v*) of pyridine. The results obtained for SCFAs did not confirm the results reported in previous studies [11,19]. In fact, the signal intensities of AA and BA increased with the use of pyridine in the reaction media. On the other hand, a decrease in the signal intensity was observed for PA when pyridine was added to the derivatization reaction. The results obtained for SCFAs standards were in accordance with the results observed for the standards containing all target analytes. An increase in the recovery values of AA was observed and high recovery values (>85 %) were achieved when all the target analytes were present, and pyridine was used in the derivatization reaction. Furthermore, even though for some of the analytes higher recovery values were obtained in the absence of pyridine, the results exhibited higher standard deviations compared to the values achieved with pyridine, which can be associated with the lack of pH control in the absence of pyridine. Considering these results, pyridine at a concentration of 6 % (*v/v*) was selected for performing the derivatization reaction in combination with 3-NPH and EDC reagents.

After establishing the concentrations for the different derivatizing reagents, the influence of using a pre-mixed reagent composite (1:1:1, *v/v/v*) or performing the individual and sequential addition of the reagents in the SCFAs reaction efficiency was assessed. Results (Fig. S11) show that the derivatization efficiency was not affected by the previous mixing of the reagents, with signal intensities similar to those obtained with the individual and sequential addition of the reagents. Thus, to simplify the procedure, a pre-mixed reagent composite was applied to perform the derivatization reaction.

In previous works, higher temperatures (>37 °C) or long reaction times (> 60 min) were needed to accomplish the derivatization reaction and provide satisfactory results using 3-NPH as a derivatizing agent [21,51]. Despite this, applying these higher temperatures could contribute to the evaporation and degradation of compounds, especially SCFAs, which are highly volatile analytes [21,51]. The temperature effect on the derivatization efficiency using a lower reaction time (30 min) was assessed. Hence, human plasma supplemented with the analytes was derivatized at temperatures of 25 and 40 °C, using the reagents concentrations and time of reaction selected before. The derivatization efficiency of all gut metabolites, except for IAA, was observed to decrease when a human plasma sample supplemented with all analytes

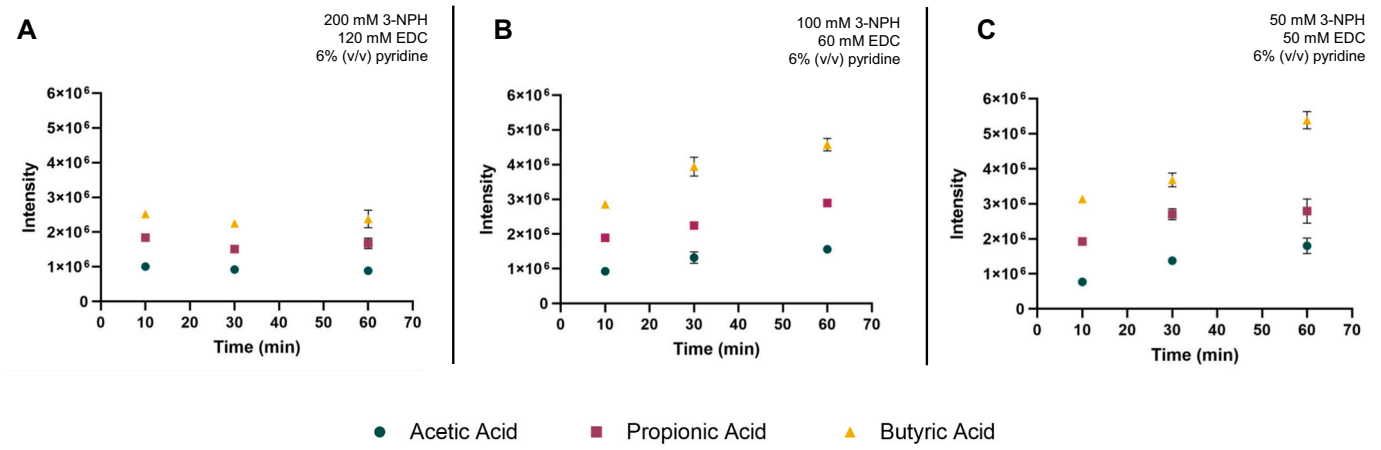

Fig. 2. Effect of the concentration of 3-NPH and EDC reagents, and reaction time on the signal intensity of SCFAs. Results obtained from the analysis of individual standard solutions of 500 μM of AA, PA and BA prepared in water, after 10, 30 and 60 min of reaction, at room temperature. (A) 200 mM 3-NPH, 120 mM EDC and 6 % (v/v) pyridine; (B) 100 mM 3-NPH, 60 mM EDC and 6 % (v/v) pyridine; (C) 50 mM 3-NPH, 50 mM EDC and 6 % (v/v) pyridine.

was derivatized at a temperature of 40 °C, as shown in Fig. 3. For the SCFAs, the decrease in derivatization efficiency (Fig. 3) was noteworthy regarding the signal intensity of the target analytes and the resulting recovery values obtained. For these metabolites, the decrease can be explained by their volatility at 40 °C. This loss of analytes would directly decrease the SCFAs available for derivatization, reducing the yield of the derivatized product. Similar results were observed for TRP, with a decrease in the signal intensity. For this compound, the results obtained could be explained by several conditions, namely, potential thermal degradation of 3-NPH, increase of side reactions, volatilization of the solvents, and potential matrix interactions.

As mentioned before, pCS and INDS were not derivatized using the proposed reaction, and they maintained their original chemical structure. However, as shown in Fig. 3, the signal of these two analytes decreased upon the increase of temperature, particularly for pCS. A decrease in the signal of INDS and pCS at a relatively mild temperature (40 °C) was somehow surprising, as these compounds are generally stable at such temperatures. Hence, slight thermal degradation, alteration of solvent properties (e.g., solvent evaporation and/or changes in solubility), and matrix effects associated with the complexity of plasma samples could be possible explanations of the obtained results. Considering all the results presented before, that demonstrate the influence of the increase of temperature on the efficiency of the derivatization reaction in real samples, a temperature of 25 °C was selected for performing the reaction to maximize the derivatization efficiency, also not affecting the signal intensity of the two underivatized analytes (pCS and INDS).

Under the best reaction conditions, comprising 200 mM 3-NPH, 120 mM EDC, 6 % (*v/v*) pyridine, and 25 °C for 30 min, all target gut metabolites yielded high derivatization efficiency and recovery values in plasma (>85 %), as well as improved peak shapes in chromatographic analysis (Fig. 4 and Fig. S12).

3.3. Method validation

Linear regression analysis was employed to establish calibration

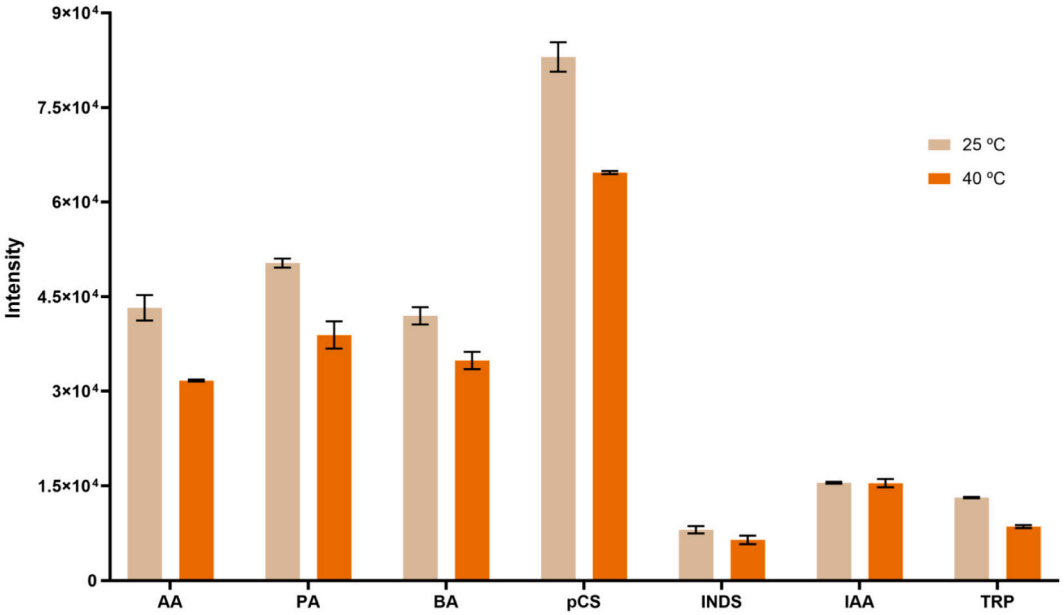

Fig. 3. Influence of the reaction temperature in the signal intensity of analytes for a pooled human plasma sample supplemented with the target analytes (500 μM of AA, PA and BA; 100 μM of pCS, INDS and IAA; 1000 μM of TRP).

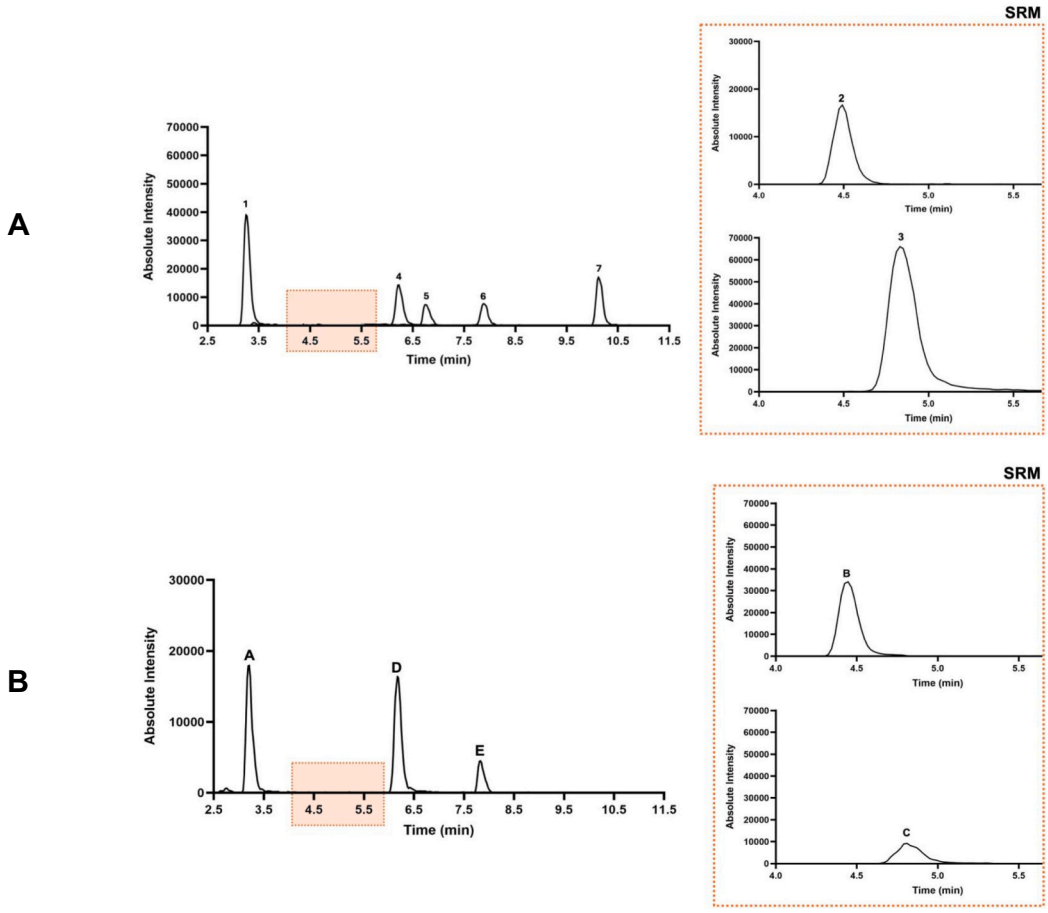

Fig. 4. Representative chromatograms of a standard solution (standard 4) of the seven gut metabolites (A) and corresponding internal standards (B) prepared in water. 1: 3-Indoxyl sulfate (INDS); 2: *p*-Cresol sulfate (pCS); 3: Acetic acid (AA); 4: Propionic acid (PA); 5: Tryptophan (TRP); 6: Butyric acid (BA); 7: Indole-3-acetic acid (IAA); Internal standards: A: [$^2H_4$]-3-Indoxyl sulfate (INDS-IS); B: [$^2H_4$]-*p*-Cresol sulfate (pCS-IS); C: [$^2H_4$]-Acetic acid (AA-IS); D: [$^2H_6$]-Propionic acid (PA-IS); E: [$^2H_5$]-Kynurenic acid (KYNA-IS).

curves plotted for peak area ratio (target gut metabolite/IS) versus target gut metabolite concentration, using calibration standards prepared in water and in pooled human plasma. The slopes of the calibration curves obtained in the two matrices were compared using the Student's *t*-test, which revealed no significant differences ($p < 0.05$), indicating no matrix effect from plasma components (Table S4). Therefore, method validation was carried out using solvent-based standards and QC samples prepared in water and in plasma. The calibration curves exhibited good linearity for all the analytes over the evaluated concentration ranges, with determination coefficients (r^2) > 0.997 for all the target gut metabolites (Table 2). Furthermore, back-calculated concentrations presented deviations within ±15 % of the nominal value, meeting the requirements of EMA and ICH guideline (results not shown) [32]. A visible acetic acid (AA) background signal was observed while analyzing zero samples prepared in water. This interference has been frequently reported in previous studies and has been associated with contamination of different sources, namely the reagents used in the derivatization procedure (e.g., pyridine), the water and organic solvents (e.g., ACN) used in the preparation of all the solutions [11,29,52]. Thus, in the impossibility to avoid these sources of AA and consequently control the background levels, a background correction was implemented through the analysis of zero samples ($n = 3$) in each run and subtraction of the corresponding analytical signal (mean of the peak area ratio of AA/IS) from all the standards and samples.

The LLOQ values (Table 2) for all the target gut metabolites were in the range of 0.4–8 μM. As can be observed in Table 2, the LLOQ values

Table 2
Target analytes, internal standard used for each analyte, corresponding linearity, and LLOQ values.

Analyte	Internal Standard	Linearity			LLOQ (μM)
		Range (μM)	Equation	r^2	
AA	[$^2H_4$]-acetic acid	6–150	$y = 0.0303x - 0.1459$	0.9990	6
PA	[$^2H_6$]-propionic acid	1–25	$y = 0.2245x + 0.1813$	0.9997	1
BA	[$^2H_6$]-propionic acid	1–25	$y = 0.0723x + 0.0894$	0.9988	1
pCS	[$^2H_4$]-*p*-cresol sulfate	8–200	$y = 0.0105x - 0.0037$	0.9991	8
INDS	[$^2H_4$]-3-indoxyl sulfate	4–100	$y = 0.0094x - 0.0044$	0.9992	4
IAA	[$^2H_5$]-kynurenic acid	0.4–10	$y = 0.1502x + 0.0093$	0.9990	0.4
TRP	[$^2H_5$]-kynurenic acid	4–100	$y = 0.0256x - 0.0204$	0.9983	4

AA, Acetic acid; PA, propionic acid; BA, butyric acid; pCS, *p*-cresol sulfate; INDS, indoxyl sulfate; IAA, indole-3-acetic acid; TRP, tryptophan; LLOQ, lower limit of quantification.

obtained for AA were higher than those obtained for the other SCFAs, which can be explained by the background levels observed in zero samples making it difficult to achieve lower LLOQ values for this gut metabolite. Moreover, INDS and pCS also presented higher LLOQ values (4 and 8 μM, respectively). However, in this case, these values were mostly associated with the high levels of these metabolites generally present in plasma samples rather than method sensitivity.

Accuracy and precision (intra- and inter-day) were assessed for the two matrices (water and plasma), as depicted in Tables 3 and 4. Four concentration levels were evaluated, including the LLOQ, within three times of the LLOQ (low QC), around the geometric mean of the calibration curve range (medium QC), and at least at 75 % of the ULOQ (high QC). For the QC samples prepared in water (Table 3), the intra- and inter-day precision and accuracy were in accordance with EMA and ICH requirements for bioanalytical assay validation [32], with precision expressed by CV not exceeding 15 % and accuracy ranging from 85 to 115 %. The intra-day precision was ≤10.3 % and the accuracy ranged between 87.0 and 114 % of the nominal concentrations of the target gut metabolites (Table 3). The inter-day determinations yielded precision values ≤13.5 % and accuracy values between 94.9 and 107 % (Table 3).

Regarding the intra- and inter-day accuracy and precision of each analyte determination in QC samples prepared in plasma (Table 4), the calculated values were also within the recommended limits established by the guidelines (CV ≤15 % and ± 15 % of the nominal concentration) [32]. Precision values ≤7.4 % and accuracy values between 90.9 and 112 % were obtained for the intra-day determinations (Table 4). For the inter-day determinations, the precision was ≤9.7 % and the accuracy ranged between 91.7 and 111 % of the nominal concentrations of the target analytes (Table 4).

The comparison of the concentrations of derivatized analytes in the QC prepared in water after 24 and 48 h storage in the autosampler evidenced that all analytes were stable in these conditions, exhibiting values ranging between 87.5 and 113.2 % of the nominal concentrations after 24 h and between 90.2 and 110.4 % after 48 h (Table S5). The target analytes also proved to be stable in the plasma matrix after 24 h in the autosampler at 6 °C, with accuracy values between 93.4 and 102 % (Table S5). These results demonstrated the adequacy of the 24 h-period used for processing and analyzing samples, ensuring accurate determinations. Additionally, no carry-over was observed when the solvent mixture ACN-H_2O (50:50, *v/v*) was analyzed after a high concentration calibration standard or each set of samples, indicating that the residual analytes remaining in the analytical instrument between injections were negligible.

3.4. Assessment of the method practicality and comparison to other methods

The practicability of the developed method was evaluated using the Blue Applicability Grade Index (BAGI), a recently developed metric tool [53]. This metric tool assesses ten attributes (Fig. 5) associated with the analytical methodology's applicability and functionality, permitting to create an asteroid pictogram with a score in the center of the graph. The result achieved using the BAGI metric is obtained through the attribution of four score points (2.5, 5.0, 7.5, and 10) to each attribute, which correspond to different colors in the pictogram, that is, white, light blue, blue, or dark blue, respectively. It should be noted that a BAGI score of 25 indicates the lowest method performance and 100 corresponds to the highest method applicability. Furthermore, for a procedure to be considered practical, an overall score of at least 60 must be achieved. The pictogram and the total score (65) obtained for the proposed multi-analyte UHPLC-MS/MS method is presented in Fig. 5. Based on the total score obtained (> 60), the newly developed method can be considered practical and feasible for bioanalytical purposes. The main features contributing to the applicability and functionality of the new method

Table 3
Intra- and inter-day accuracy and precision of the method for the determination of the target gut metabolites in QC samples prepared in water.

Analyte	Nominal concentration (μM)	Intra-day			Inter-day		
		Measured concentration			Measured concentration		
		Mean (μM)	Accuracy (%)	CV (%)	Mean (μM)	Accuracy (%)	CV (%)
AA	6	6.7	112	10.3	6.1	101	10.4
	15	14.8	98.6	3.3	15.9	106	6.3
	60	58.3	97.2	1.5	58.5	97.5	1.4
	120	121	101	0.7	119	99.1	1.8
PA	1	0.87	87.0	2.7	0.98	97.8	13.5
	2.5	2.6	103	2.3	2.6	104	3.7
	10	10.1	101	1.1	9.9	99.4	1.9
	20	19.9	99.4	1.2	19.7	98.6	1.6
BA	1	0.87	87.0	5.6	0.95	94.9	11.8
	2.5	2.5	99.4	3.3	2.5	98.7	1.5
	10	10.2	103	1.3	10.0	100	3.4
	20	20.4	102	0.4	20.2	101	1.0
pCS	8	8.1	101	1.7	7.9	98.7	4.2
	20	19.8	99.1	0.6	20.2	101	2.4
	80	78.6	98.3	2.2	79.0	98.8	1.0
	160	165	103	1.0	161	101	2.1
INDS	4	4.6	114	3.0	4.0	101	11.2
	10	10.3	103	4.6	10.3	103	5.8
	40	39.4	98.6	2.0	40.0	100	2.3
	80	79.8	99.8	0.5	79.9	99.9	1.7
IAA	0.4	0.45	114	2.8	0.42	106	12.1
	1	1.0	103	2.9	1.1	107	5.1
	4	3.7	93.2	2.2	3.8	95.4	2.3
	8	8.2	102	0.1	8.1	101	1.3
TRP	4	4.5	114	5.4	4.2	107	12.0
	10	9.6	95.7	0.4	10.1	101	11.2
	40	40.7	102	1.5	39.7	99.2	4.0
	80	79.2	99.0	0.6	79.8	99.8	0.7

AA, Acetic acid; PA, propionic acid; BA, butyric acid; pCS, *p*-cresol sulfate; INDS, indoxyl sulfate; IAA, indole-3-acetic acid; TRP, tryptophan; CV, coefficient of variation.

Table 4
Intra- and inter-day accuracy and precision of the method for the determination of the target gut metabolites in QC samples prepared in human plasma.

Analyte	Nominal concentration (μM)	Intra-day			Inter-day		
		Measured concentration			Measured concentration		
		Mean (μM)	Accuracy (%)	CV (%)	Mean (μM)	Accuracy (%)	CV (%)
AA	6	6.5	109	7.4	6.7	111	3.3
	15	15.2	101	4.6	15.1	101	0.6
	60	60.1	100	1.8	60.1	100	0.1
	120	116	96.8	0.3	117	97.7	1.2
PA	1	1.0	104	6.5	0.97	97.2	9.7
	2.5	2.4	96.4	2.5	2.4	96.9	0.7
	10	9.9	99.3	5.4	10.4	104	6.2
	20	21.6	108	2.8	21.3	106	2.1
BA	1	1.1	107	6.2	1.0	102	5.6
	2.5	2.4	97.8	2.5	2.4	95.3	3.7
	10	9.3	92.5	4.8	9.2	91.7	1.3
	20	19.7	98.3	0.8	19.8	98.8	0.7
pCS	8	9.0	112	3.8	8.5	106	8.1
	20	20.5	103	4.6	20.3	101	1.6
	80	80.3	100	1.7	80.6	101	0.5
	160	160	100	1.0	159	99.4	1.0
INDS	4	4.1	102	2.9	4.1	103	1.7
	10	10.4	104	2.6	10.1	101	4.9
	40	40.3	101	1.0	40.2	100	0.5
	80	80.1	100	2.2	80.1	100	0.1
IAA	0.4	0.39	98.3	6.1	0.39	97.9	0.6
	1	0.91	90.9	2.7	0.93	93.1	3.4
	4	3.7	93.1	4.5	3.9	98.4	7.6
	8	7.2	90.0	2.7	7.4	92.5	3.8
TRP	4	4.0	99.8	3.6	3.9	98.1	2.2
	10	10.2	102	2.7	10.0	100	2.8
	40	38.7	96.7	2.5	40.2	100	5.1
	80	80.5	101	2.5	79.5	99.4	1.7

AA, Acetic acid; PA, propionic acid; BA, butyric acid; pCS, *p*-cresol sulfate; INDS, indoxyl sulfate; IAA, indole-3-acetic acid; TRP, tryptophan; CV, coefficient of variation.

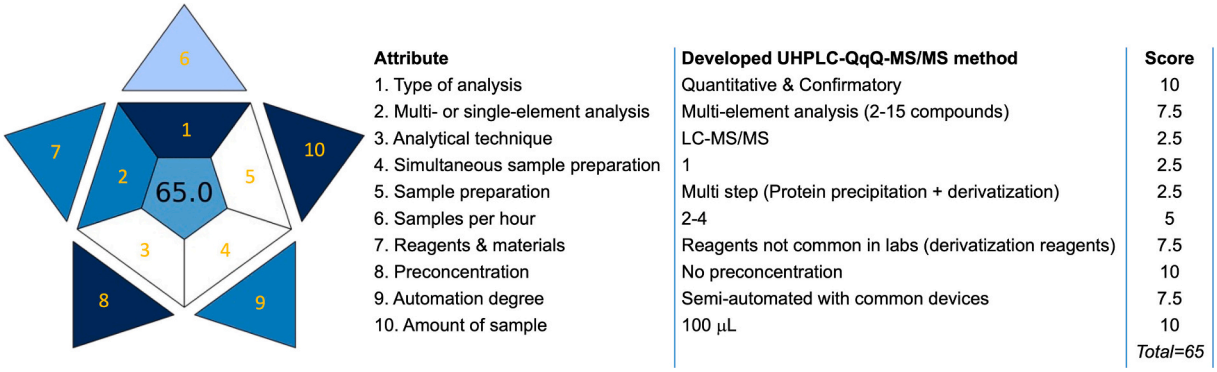

Fig. 5. Evaluation of the multi-analyte UHPLC-QqQ-MS/MS method developed for the determination of gut metabolites in plasma using the BAGI metric tool.

included the implementation of a quantitative and confirmatory analysis (attribute 1), which allows the identification and subsequent quantification of the analyte and can be a significant advantage in bioanalysis applications. Furthermore, the reduced amount of sample used (100 μL) (attribute 10), without the need to implement a preconcentration step (attribute 8), were features that improved the practicality of the proposed methodology and are particularly relevant in the analysis of biological samples. On the other hand, the main attributes contributing to decrease the overall score were the use of LC-MS/MS as analytical technique (attribute 3), and the implementation of a multi-step sample preparation procedure (attribute 5) that only allows the pre-treatment of one sample at a time (attribute 4). Considering the last three attributes mentioned, it is important to note that only attribute 4 could be further modified to improve the practicality of the method by the application of sample preparation procedures that allow simultaneous treatment of more than one sample, for instance, through the implementation of protein precipitation in the 96-well format.

Compared to previously reported methods for the determination of the target gut-metabolites in plasma samples [19,20,24,52], the proposed method offers significant advantages. Firstly, the ability to simultaneously analyze non-derivatized (pCS and INDS) and derivatized (SCFAs, IAA, and TRP) metabolites without compromising their analyses represents an advance over previous methods, allowing the quantification of metabolites with different physicochemical properties in a single run. In fact, pCS and INDS, two relevant intestinal metabolites implicated in the development of several diseases, such as chronic kidney disease (CKD) and cardiovascular disorders [22,54], are not commonly analyzed simultaneously with the other target analytes, fostering research upon their relation in disease progression and microbiome metabolites. Furthermore, the chemical derivatization procedure

implemented here presents some advantages compared to previous methods using the same derivatization reagent (3-NPH). Generally, for other methods, the temperature and the reaction time were higher than 30 °C and 60 min, respectively [19,20,24,52]. On the other hand, the proposed method uses a temperature of 25 °C and requires only 30 min to perform the derivatization reaction, allowing a faster and more stable reaction, reducing the risk of possible degradation or evaporation of some metabolites, particularly SCFAs. In fact, in previous works that analyze only SCFAs, to avoid their evaporation, the reaction has been carried out at lower temperatures, usually 4 °C, but with an increase in reaction time that can reach more than 4 h [20,52]. Thus, the proposed method allows the simultaneous derivatization of different gut metabolites by combining reaction conditions that make the process faster and more efficient. The LLOQ values obtained in the current work were in the low μM range (≤ 8 μM for all the analytes), which were in accordance with the previous reports to determine the target analytes in plasma samples [19,20,24,52].

3.5. Application to clinical samples

The validated UHPLC-MS/MS method was ultimately applied to the determination of the target gut metabolites content in human plasma samples obtained from children (samples 1 to 5) and adults (samples 6 to 10) participating in two clinical studies (see section 2.3.4 for more detail) to evaluate its adequacy for application in clinical samples. Out of the five children plasma samples, two were retrieved from children with ADHD (samples 1 and 2) and three were obtained from healthy children (samples 3, 4 and 5). The five plasma samples obtained from adults corresponded to healthy individuals (samples 6 to 10). The results obtained for each sample ($n = 2$) are presented in Table 5 along with illustrative chromatograms of two plasma samples, one from a child (Fig. 6A) and one from an adult individual (Fig. 6B). For confirmatory analysis of the target analytes in samples, a system based on four identification points (1 precursor ion and 2 product ions) was applied.

Table 5
Quantification of target gut metabolites in plasma samples collected from children and adult individuals participating in clinical studies.

Plasma samples[a]	Gut metabolite concentration (μM)						
	AA	PA	BA	pCS	INDS	IAA	TRP
Sample 1	40.0 ± 0.2	1.22 ± 0.03	0.3 ± 0.1*	4.9 ± 0.2*	2.2 ± 0.1*	0.4 ± 0.1	52 ± 1
Sample 2	59.5 ± 0.4	1.1 ± 0.2	0.7 ± 0.1*	115 ± 1	6 ± 1	0.64 ± 0.01	49.6 ± 0.3
Sample 3	82.1 ± 1.3	1.5 ± 0.1	1.1 ± 0.1	52.8 ± 0.1	5.6 ± 0.4	1.3 ± 0.1	50.9 ± 0.3
Sample 4	39.1 ± 0.3	1.06 ± 0.02	0.06 ± 0.01*	59 ± 1	4.7 ± 0.1	0.87 ± 0.04	57 ± 1
Sample 5	55.7 ± 0.4	5.5 ± 0.4	5.0 ± 0.1	57 ± 1	3.46 ± 0.02	1.2 ± 0.1	49 ± 1
Sample 6	120 ± 1	2.3 ± 0.2	1.6 ± 0.1	101 ± 1	14.1 ± 0.3	0.9 ± 0.1	35 ± 1
Sample 7	64 ± 1	1.7 ± 0.1	0.7 ± 0.1*	36.2 ± 0.4	7.6 ± 0.1	1.4 ± 0.1	42.7 ± 0.4
Sample 8	37.1 ± 0.4	1.5 ± 0.1	0.3 ± 0.1*	86 ± 1	7.0 ± 0.4	6.5 ± 0.2	64 ± 1
Sample 9	80.2 ± 0.4	1.44 ± 0.04	0.28 ± 0.09*	133 ± 2	1.2 ± 0.2*	0.32 ± 0.03*	41 ± 2
Sample 10	78 ± 2	2.2 ± 0.2	0.3 ± 0.1*	182 ± 1	6.4 ± 0.1	1.5 ± 0.1	31 ± 1

AA, Acetic acid; PA, propionic acid; BA, butyric acid; pCS, *p*-cresol sulfate; INDS, indoxyl sulfate; IAA, indole-3-acetic acid; TRP, tryptophan.
[a] Samples were collected from children (sample 1 to 5) and adults (sample 6 to 10). Please see the text for more detail.
* < LLOQ (1 μM for BA; 8 μM for pCS; 4 μM for INDS; 0.4 μM for IAA).

Qualifier (q) and quantifier (Q) ions relative abundance was determined in standards prepared in water and in plasma samples, with the maximum permitted tolerances of ±20 % for AA, BA, INDS and IAA as the q/Q values were ≥ 50 %, ± 25 % for TRP because the q/Q values belong to the range 20–50 %, and ± 50 % for PA and pCS as the q/Q values were ≤ 10 % [55]. The standards prepared in water presented mean ion ratio values of 80.0 ± 1.7 % for AA, 1.6 ± 0.2 % for PA, 51.6 ± 3.4 % for BA, 9.1 ± 0.8 % for pCS, 95.4 ± 3.3 % for INDS, 84.6 ± 5.8 % for IAA, and 38.0 ± 1.7 % for TRP (Table S6). In the case of plasma samples, mean ion ratio values of 80.3 ± 2.3 % for AA, 2.0 ± 0.2 % for PA, 47.2 ± 3.0 % for BA, 8.9 ± 0.7 % for pCS, 87.7 ± 7.9 % for INDS, 86.8 ± 4.9 % for IAA, and 40.7 ± 3.0 % for TRP were obtained (Table S7). Therefore, these results show that ion ratio values complied with the tolerance limits in all samples and allowed to confirm the presence of all the target gut metabolites in the analyzed plasma samples.

As shown in Table 5, all the target gut metabolites were successfully detected and quantified in the analyzed plasma samples, except for BA which was present in quantities below the LLOQ (<1 μM) in seven out of ten samples. Moreover, sample 1 and sample 9 exhibited pCS, INDS, and/or IAA levels below the LLOQ (<8, 4 and 0.4 μM, respectively). The concentrations determined for each analyte were variable, with the higher concentrations found for AA (37.1–120 μM), pCS (4.9–182 μM), and TRP (31–64 μM). On the other hand, the lowest concentrations were observed for PA (1.1–5.5 μM), BA (0.06–5.0 μM), and IAA (0.32–6.5 μM). Additionally, the results indicate that the proposed methodology was suitable for the quantification of the target analytes across a broad range of concentrations and was applicable to the analysis of plasma samples from both pediatric and adult individuals. The comparison of the results obtained for the two groups of individuals under study indicated similar concentration levels in children and in adults, for all the target gut metabolites (Table 5, Fig. 6A and B). Furthermore, the concentrations found for all the analytes were in accordance with the values reported in the literature [3,19,30,54,56]. These observations are illustrated by the results achieved for the three determined SCFAs, which are the most abundant SCFAs in humans, with predominance of AA [57,58]. The results obtained were consistent with this observation, with the higher concentrations (37.1–120 μM) obtained for AA and the lower and similar concentrations found for PA (1.1–5.5 μM) and BA (0.06–5.0 μM).

4. Conclusion

A liquid chromatography method coupled with tandem mass spectrometry detection was successfully developed and validated for the simultaneous quantification of seven gut metabolites in human plasma samples. A chemical derivatization procedure using 3-nitrophenylhydrazine hydrochloride that enables highly sensitive detection of the target analytes, particularly SCFAs, was applied after a simple, rapid and low-cost sample treatment involving protein precipitation with acetonitrile and the use of reduced sample volumes (100 μL). After studying the derivatization and UHPLC−MS/MS separative and detection conditions, the proposed method was validated and applied to real samples, demonstrating to be sensitive, selective, accurate, and precise for the quantitative analysis of the seven target gut metabolites in human plasma samples, in a wide concentration range. LLOQ values obtained for all the analytes were in the lower μM range, being similar or even lower than values reported in previous studies [3,19,30,54,56]. Additionally, application of the proposed method to the analysis of clinical human plasma samples from both children and adults was successfully achieved. Finally, the method practicability was demonstrated by a favorable BAGI score of 65, which evidenced the potential of the proposed methodology to be applied in bioanalytical studies.

Moreover, this new analytical method can be regarded as a significant advance in the state of the art of gut microbiota studies due to the simultaneous quantification of different groups of gut metabolites that

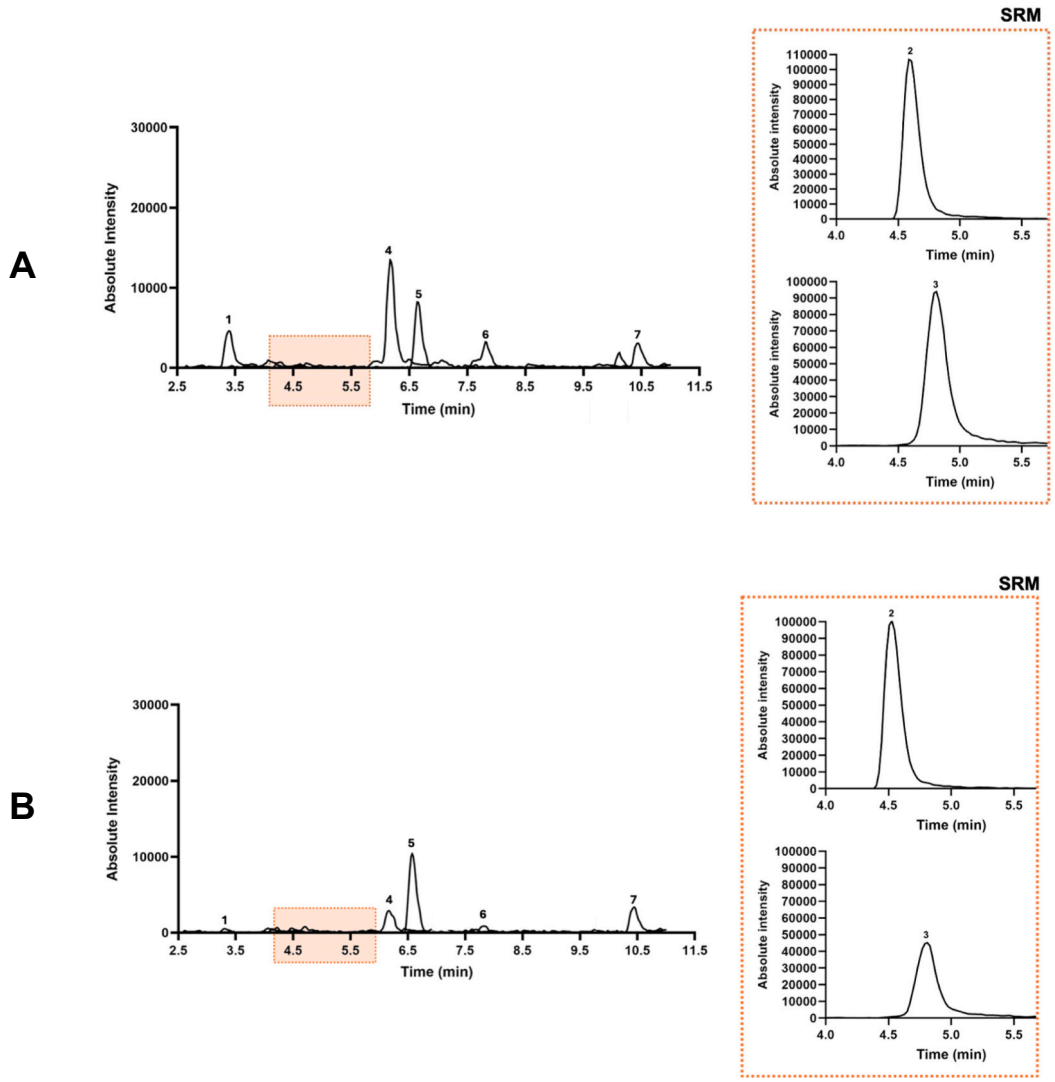

Fig. 6. Representative chromatograms of a plasma sample from a child (A) and a plasma sample from an adult individual (B). 1: 3-Indoxyl sulfate (INDS); 2: *p*-Cresol sulfate (pCS); 3: Acetic acid (AA); 4: Propionic acid (PA); 5: Tryptophan (TRP); 6: Butyric acid (BA); 7: Indole-3-acetic acid (IAA).

were commonly determined separately, namely SCFAs in combination with amino acids and their derivatives (e.g., pCS and TRP). Thus, the application of the proposed method may valuably contribute to a better understanding of the impact of the gut metabolites in the health-to-disease transition. Furthermore, the methodology shows the potential to be adapted and applied to the analysis of other types of biomatrices, namely non-invasive samples (e.g., urine). With further optimization, namely in the derivatization and chromatographic procedures, it can be extended to the analysis of other metabolites, permitting to obtain a metabolic fingerprint that contributes to a more comprehensive elucidation of gut microbial metabolism and its impact on human health.

CRediT authorship contribution statement

Sara R. Fernandes: Writing – original draft, Validation, Methodology, Investigation. **Cristian Azorín:** Writing – review & editing, Investigation. **Eduarda M.P. Silva:** Writing – review & editing, Formal analysis. **Manuel Miró:** Writing – review & editing, Supervision, Project administration. **Luisa Barreiros:** Writing – review & editing, Supervision, Funding acquisition, Formal analysis, Conceptualization. **Marcela A. Segundo:** Writing – review & editing, Supervision, Resources, Project administration, Funding acquisition, Conceptualization.

Declaration of competing interest

The authors declare that they have no known competing financial interests or personal relationships that could have appeared to influence the work reported in this paper.

Acknowledgements

This work received financial support from PT national funds (FCT/MECI, Fundação para a Ciência e Tecnologia and Ministério da Educação, Ciência e Inovação) through the project UID/50006-Laboratório Associado para a Química Verde - Tecnologias e Processos Limpos. S. R. Fernandes thanks FCT and ESF (European Social Fund) through Norte 2020 (Programa Operacional Regional Norte) for her PhD grants SFRH/BD/130948/2017 and COVID/BD/152406/2022 (DOI https://doi.org/10.54499/COVID/BD/152406/2022). C. Azorín also thanks the Spanish Ministry of Universities for both his predoctoral and mobility grants (FPU19/04239 and EST23/00601). L. Barreiros acknowledges funding from FCT through program DL 57/2016 – Norma transitória. M. Miró acknowledges financial support from the Spanish Ministry of Science and Innovation (MCIN) and Spanish State Research Agency (AEI) through projects PID2020-117686RB-C33-R and PID2024-156804OB-

C33 (MCIN/AEI/10.13039/501100011033). The authors acknowledge Benedita Sampaio-Maia (FMDUP, i3S), principal investigator of the project Microbi-A, and Joana Ferreira-Gomes (FMUP), principal investigator of the project M2Child, for aiding in the provision of plasma samples. The authors would also like to thank Carolina Costa, Teresa Correia de Sá, Diana R. Cunha and Andreia N. Meireles for their help in collecting and processing samples for analysis. Authors are also grateful to Artur M. S. Silva, Maria da Graça P. M. S. Neves (University of Aveiro), Alberto Chisvert, and Juan L. Benedé (University of Valencia), for helpful suggestions and stimulating discussions related to the fragmentation mechanisms and to chromatographic analysis.

Appendix A. Supplementary data

Supplementary data to this article can be found online at https://doi.org/10.1016/j.jchromb.2025.124764.

Data availability

Data will be made available on request.

References

[1] Q. Fang, N. Liu, B.J. Zheng, F. Guo, X.C. Zeng, X.Y. Huang, D.S. Ouyang, Roles of gut microbial metabolites in diabetic kidney disease, Front. Endocrinol. 12 (2021) 636175, https://doi.org/10.3389/fendo.2021.636175.
[2] K.A. Krautkramer, J. Fan, F. Backhed, Gut microbial metabolites as multi-kingdom intermediates, Nat. Rev. Microbiol. 19 (2021) 77–94, https://doi.org/10.1038/s41579-020-0438-4.
[3] L.N. Zhou, D. Yu, S.J. Zheng, R.Z. Ouyang, Y.T. Wang, G.W. Xu, Gut microbiota-related metabolome analysis based on chromatography-mass spectrometry, TrAC Trends Anal. Chem. 143 (2021) 116375, https://doi.org/10.1016/j.trac.2021.116375.
[4] A. Agus, J. Planchais, H. Sokol, Gut microbiota regulation of tryptophan metabolism in health and disease, Cell Host Microbe 23 (2018) 716–724, https://doi.org/10.1016/j.chom.2018.05.003.
[5] A. Lavelle, H. Sokol, Gut microbiota-derived metabolites as key actors in inflammatory bowel disease, Nat. Rev. Gastroenterol. Hepatol. 17 (2020) 223–237, https://doi.org/10.1038/s41575-019-0258-z.
[6] S. Han, E.R. Guiberson, Y. Li, J.L. Sonnenburg, High-throughput identification of gut microbiome-dependent metabolites, Nat. Protoc. 19 (2024) 2180–2205, https://doi.org/10.1038/s41596-024-00980-6.
[7] J. Roach, R. Mital, J.J. Haffner, N. Colwell, R. Coats, H.M. Palacios, Z. Liu, J.L. P. Godinho, M. Ness, T. Peramuna, L.-I. McCall, Microbiome metabolite quantification methods enabling insights into human health and disease, Methods 222 (2024) 81–99, https://doi.org/10.1016/j.ymeth.2023.12.007.
[8] F. Brial, A. Le Lay, M.E. Dumas, D. Gauguier, Implication of gut microbiota metabolites in cardiovascular and metabolic diseases, Cell. Mol. Life Sci. 75 (2018) 3977–3990, https://doi.org/10.1007/s00018-018-2901-1.
[9] E.P. Nyangale, D.S. Mottram, G.R. Gibson, Gut microbial activity, implications for health and disease: the potential role of metabolite analysis, J. Proteome Res. 11 (2012) 5573–5585, https://doi.org/10.1021/pr300637d.
[10] J. Tan, C. McKenzie, M. Potamitis, A.N. Thorburn, C.R. Mackay, L. Macia, Chapter three - the role of short-chain fatty acids in health and disease, in: F.W. Alt (Ed.), Advances in Immunology, Academic Press, 2014, pp. 91–119.
[11] M.F. Zeng, H.C. Cao, Fast quantification of short chain fatty acids and ketone bodies by liquid chromatography-tandem mass spectrometry after facile derivatization coupled with liquid-liquid extraction, J. Chromatogr. B. 1083 (2018) 137–145, https://doi.org/10.1016/j.jchromb.2018.02.040.
[12] N. Trivedi, H.E. Erickson, V. Bala, Y.S. Chhonker, D.J. Murry, A concise review of liquid chromatography-mass spectrometry-based quantification methods for short chain fatty acids as endogenous biomarkers, Int. J. Mol. Sci. 23 (2022) 13486, https://doi.org/10.3390/ijms232113486.
[13] I. Cervenka, L.Z. Agudelo, J.L. Ruas, Kynurenines: tryptophan's metabolites in exercise, inflammation, and mental health, Science 357 (2017) eaaf9794, https://doi.org/10.1126/science.aaf9794.
[14] B. Sampaio-Maia, L. Simoes-Silva, M. Pestana, R. Araujo, I.J. Soares-Silva, The role of the gut microbiome on chronic kidney disease, in: S. Sariaslani, G.M. Gadd (Eds.), Advances in Applied Microbiology vol. 96, Elsevier Academic Press Inc, San Diego, 2016, pp. 65–94.
[15] C.A. Falconi, C.V.C. Junho, F. Fogaça-Ruiz, I.C.S. Vernier, R.S. Cunha, A.E. M. Stinghen, M.S. Carneiro-Ramos, Uremic toxins: an alarming danger concerning the cardiovascular system, Front. Physiol. 12 (2021) 686249, https://doi.org/10.3389/fphys.2021.686249.
[16] R. Vanholder, A. Pletinck, E. Schepers, G. Glorieux, Biochemical and clinical impact of organic uremic retention solutes: a comprehensive update, Toxins 10 (2018) 1–5733, https://doi.org/10.3390/toxins10010033.
[17] A.L. Graboski, M.R. Redinbo, Gut-derived protein-bound uremic toxins, Toxins 12 (2020) 590, https://doi.org/10.3390/toxins12090590.
[18] P. Chalova, A. Tazky, L. Skultety, L. Minichova, M. Chovanec, S. Ciernikova, P. Mikus, J. Piestansky, Determination of short-chain fatty acids as putative biomarkers of cancer diseases by modern analytical strategies and tools: a review, Front. Oncol. 13 (2023) 1110235, https://doi.org/10.3389/fonc.2023.1110235.
[19] H. Liao, C. Wang, C. Lee, H. Kao, W. Wu, C. Kuo, Development of an efficient and sensitive chemical derivatization-based LC–MS/MS method for quantifying gut microbiota-derived metabolites in human plasma and its application in studying cardiovascular disease, J. Proteome Res. 20 (2021) 3508–3518, https://doi.org/10.1021/acs.jproteome.1c00147.
[20] W. Song, H. Park, S. Kim, S. Jo, B. Kim, A.B. Theberge, Y. Kim, Chemical derivatization-based LC–MS/MS method for quantitation of gut microbial short-chain fatty acids, J. Ind. Eng. Chem. 83 (2020) 297–302, https://doi.org/10.1016/j.jiec.2019.12.001.
[21] T. Jankech, I. Gerhardtova, P. Majerova, J. Piestansky, J. Jampilek, A. Kovac, Derivatization of carboxylic groups prior to their LC analysis – a review, Anal. Chim. Acta 1300 (2024) 342435, https://doi.org/10.1016/j.aca.2024.342435.
[22] S.R. Fernandes, A.N. Meireles, S.S. Marques, L. Silva, L. Barreiros, B. Sampaio-Maia, M. Miró, M.A. Segundo, Sample preparation and chromatographic methods for the determination of protein-bound uremic retention solutes in human biological samples: An overview, J. Chromatogr. B Analyt. Technol. Biomed. Life Sci. 1215 (2023) 123578, https://doi.org/10.1016/j.jchromb.2022.123578.
[23] I. Sadok, A. Gamian, M.M. Staniszewska, Chromatographic analysis of tryptophan metabolites, J. Sep. Sci. 40 (2017) 3020–3045, https://doi.org/10.1002/jssc.201700184.
[24] H. Xu, J. Wang, Y. Liu, Y. Wang, X. Zhong, C. Li, K. Wang, X. Guo, C. Xie, Development of a simultaneous quantification method for the gut microbiota-derived core nutrient metabolome in mice and its application in studying host-microbiota interaction, Anal. Chim. Acta 1251 (2023) 341039, https://doi.org/10.1016/j.aca.2023.341039.
[25] H.K. Krishnamurthy, M. Pereira, J. Bosco, J. George, V. Jayaraman, K. Krishna, T. Wang, K. Bei, J.J. Rajasekaran, Gut commensals and their metabolites in health and disease, Front. Microbiol. 14 (2023) 1244293, https://doi.org/10.3389/fmicb.2023.1244293.
[26] A. Gold, J. Zhu, Not just a gut feeling: a deep exploration of functional bacterial metabolites that can modulate host health, Gut Microbes 14 (2022) 2125734, https://doi.org/10.1080/19490976.2022.2125734.
[27] L. Liu, J.R. Huh, K. Shah, Microbiota and the gut-brain-axis: implications for new therapeutic design in the CNS, eBioMedicine 77 (2022), https://doi.org/10.1016/j.ebiom.2022.103908.
[28] L.H. Morais, H.L. Schreiber, S.K. Mazmanian, The gut microbiota–brain axis in behaviour and brain disorders, Nat. Rev. Microbiol. 19 (2021) 241–255, https://doi.org/10.1038/s41579-020-00460-0.
[29] C.C. Weng, C. Suarez, S.E. Cheang, G. Couture, M.L. Goodson, M. Barboza, K. M. Kalanetra, C.F. Masarweh, D.A. Mills, H.E. Raybould, C.B. Lebrilla, Quantifying gut microbial short-chain fatty acids and their isotopomers in mechanistic studies using a rapid, readily expandable LC–MS platform, Anal. Chem. 96 (2024) 2415–2424, https://doi.org/10.1021/acs.analchem.3c04352.
[30] Z. Chen, Z. Gao, Y. Wu, R. Shrestha, H. Imai, N. Uemura, K.-i. Hirano, H. Chiba, S.-P. Hui, Development of a simultaneous quantitation for short-, medium-, long-, and very long-chain fatty acids in human plasma by 2-nitrophenylhydrazine-derivatization and liquid chromatography–tandem mass spectrometry, J. Chromatogr. B. 1126 (2019) 121771, https://doi.org/10.1016/j.jchromb.2019.121771.
[31] M. Dei Cas, R. Paroni, A. Saccardo, E. Casagni, S. Arnoldi, V. Gambaro, M. Saresella, C. Mario, F. La Rosa, I. Marventano, F. Piancone, G. Roda, A straightforward LC-MS/MS analysis to study serum profile of short and medium chain fatty acids, J. Chromatogr. B 1154 (2020) 121982, https://doi.org/10.1016/j.jchromb.2020.121982.
[32] European Medicines Agency, ICH guideline M10 on bioanalytical method validation and study sample analysis EMA/CHMP/ICH/172948/2019, 2023.
[33] S. Zhao, L. Li, Chemical derivatization in LC-MS-based metabolomics study, TrAC Trends Anal. Chem. 131 (2020) 115988, https://doi.org/10.1016/j.trac.2020.115988.
[34] V. David, S.C. Moldoveanu, T. Galaon, Derivatization procedures and their analytical performances for HPLC determination in bioanalysis, Biomed. Chromatogr. 35 (2021) e5008, https://doi.org/10.1002/bmc.5008.
[35] L. Barreiros, E.M.P. Silva, I.S. Alencastre, M. Lamghari, M.A. Segundo, Determination of neuropeptide Y Y1 receptor antagonist BIBP 3226 and evaluation of receptor expression based on liquid chromatography coupled with tandem mass spectrometry, Anal. Bioanal. Chem. 412 (2020) 6625–6632, https://doi.org/10.1007/s00216-020-02825-z.
[36] L. Barreiros, J.L. Amoreira, S. Machado, S.R. Fernandes, E.M.P. Silva, P. Sá, S. Kietaibl, M.A. Segundo, Determination of tranexamic acid in human plasma by UHPLC coupled with tandem mass spectrometry targeting sub-microgram per milliliter levels, Microchem. J. 144 (2019) 144–150, https://doi.org/10.1016/j.microc.2018.08.061.
[37] E.M.P. Silva, L. Barreiros, S.R. Fernandes, P. Sá, J.P.P. Ramalho, M.A. Segundo, Acetonitrile adducts of tranexamic acid as sensitive ions for quantification at residue levels in human plasma by UHPLC-MS/MS, Pharmaceuticals 14 (2021) 1205, https://doi.org/10.3390/ph14121205.
[38] E.M.P. Silva, P.A.M.M. Varandas, T. Melo, C. Barros, I.S. Alencastre, L. Barreiros, P. Domingues, M. Lamghari, M.R.M. Domingues, M.A. Segundo, Gas-phase structural characterization of neuropeptides Y Y1 receptor antagonists using mass spectrometry: Orbitrap vs triple quadrupole, J. Pharm. Biomed. Anal. 151 (2018) 227–234, https://doi.org/10.1016/j.jpba.2018.01.013.
[39] D.P. Demarque, A.E.M. Crotti, R. Vessecchi, J.L.C. Lopes, N.P. Lopes, Fragmentation reactions using electrospray ionization mass spectrometry: an

important tool for the structural elucidation and characterization of synthetic and natural products, Nat. Prod. Rep. 33 (2016) 432–455, https://doi.org/10.1039/C5NP00073D.
[40] O. Hodek, J. Henderson, L. Argemi-Muntadas, A. Khan, T. Moritz, Structural elucidation of 3-nitrophenylhydrazine derivatives of tricarboxylic acid cycle acids and optimization of their fragmentation to boost sensitivity in liquid chromatography-mass spectrometry, J. Chromatogr. B 1222 (2023) 123719, https://doi.org/10.1016/j.jchromb.2023.123719.
[41] W.M.A. Niessen, Tandem mass spectrometry of organic nitro and halogen compounds: competition between losses of molecules and of radicals, Int. J. Mass Spectrom. 460 (2021) 116496, https://doi.org/10.1016/j.ijms.2020.116496.
[42] C.C.J. Fitzgerald, R. Hedman, D.R. Uduwela, B. Paszerbovics, A.J. Carroll, T. Neeman, A. Cawley, L. Brooker, M.D. McLeod, Profiling urinary sulfate metabolites with mass spectrometry, Front. Mol. Biosci. 9 (2022) 829511, https://doi.org/10.3389/fmolb.2022.829511.
[43] Y. Yan, D.L. Rempel, T.E. Holy, M.L. Gross, Mass spectrometry combinations for structural characterization of sulfated-steroid metabolites, J. Am. Soc. Mass Spectrom. 25 (2014) 869–879, https://doi.org/10.1007/s13361-014-0836-9.
[44] A. Lafaye, C. Junot, B. Ramounet-Le Gall, P. Fritsch, E. Ezan, J.-C. Tabet, Profiling of sulfoconjugates in urine by using precursor ion and neutral loss scans in tandem mass spectrometry. Application to the investigation of heavy metal toxicity in rats, J. Mass Spectrom. 39 (2004) 655–664, https://doi.org/10.1002/jms.635.
[45] A. Rifai, S. Bourcier, D. Arquier, Y. Charvet, F. Jaber, G. Bouchoux, Fragmentation reactions of phenoxide anions: deprotonated Dinoterb and related structures, J. Mass Spectrom. 46 (2011) 1079–1088, https://doi.org/10.1002/jms.1991.
[46] T. Fukushima, M. Umino, T. Sakamoto, M. Onozato, A review of chromatographic methods for bioactive tryptophan metabolites, kynurenine, kynurenic acid, quinolinic acid, and others, in biological fluids, Biomed. Chromatogr. 36 (2022) e5308, https://doi.org/10.1002/bmc.5308.
[47] H.E. Schwartz-Zimmermann, M. Hündler, N. Reiterer, S. Ricci, R. Rivera-Chacon, E. Castillo-Lopez, Q. Zebeli, F. Berthiller, Comparison of LC-MS-based methods for the determination of carboxylic acids in animal matrices, Anal. Bioanal. Chem. 416 (2024) 1199–1215, https://doi.org/10.1007/s00216-023-05113-8.
[48] J.C.Y. Chan, D.Y.Q. Kioh, G.C. Yap, B.W. Lee, E.C.Y. Chan, A novel LCMSMS method for quantitative measurement of short-chain fatty acids in human stool derivatized with 12C- and 13C-labelled aniline, J. Pharm. Biomed. Anal. 138 (2017) 43–53, https://doi.org/10.1016/j.jpba.2017.01.044.
[49] M.J. McKay, M. Castaneda, S. Catania, K.A. Charles, E. Shanahan, S.J. Clarke, A. Engel, P. Varelis, M.P. Molloy, Quantification of short-chain fatty acids in human stool samples by LC-MS/MS following derivatization with aniline analogues, J. Chromatogr. B 1217 (2023) 123618, https://doi.org/10.1016/j.jchromb.2023.123618.
[50] R. Nagatomo, A. Ichikawa, H. Kaneko, K. Inoue, Comparison of 3-nitrophenylhydrazine, O-benzyl hydroxylamine, and 2-picolylamine derivatizations for analysis of short-chain fatty acids through liquid chromatography coupled with tandem mass spectrometry, Anal. Sci. 40 (2024) 843–851, https://doi.org/10.1007/s44211-023-00474-7.
[51] L. Yang, J. Yuan, B. Yu, S. Hu, Y. Bai, Sample preparation for fatty acid analysis in biological samples with mass spectrometry-based strategies, Anal. Bioanal. Chem. 416 (2024) 2371–2387, https://doi.org/10.1007/s00216-024-05185-0.
[52] R. Fristedt, V. Ruppert, T. Trower, J. Cooney, R. Landberg, Quantitation of circulating short-chain fatty acids in small volume blood samples from animals and humans, Talanta 272 (2024) 9125743, https://doi.org/10.1016/j.talanta.2024.125743.
[53] N. Manousi, W. Wojnowski, J. Płotka-Wasylka, V. Samanidou, Blue applicability grade index (BAGI) and software: a new tool for the evaluation of method practicality, Green Chem. 25 (2023) 7598–7604, https://doi.org/10.1039/D3GC02347H.
[54] S.R. Fernandes, L. Barreiros, B. Sampaio-Maia, M. Miró, M.A. Segundo, Total analysis system for the determination of uremic toxins in human plasma based on bead injection solid phase extraction hyphenated to mass spectrometry, Anal. Chim. Acta 1277 (2023) 341668, https://doi.org/10.1016/j.aca.2023.341668.
[55] European Commission, European Union decision 2002/657/EC 17.08.2002: commission decision laying down performance criteria for the analytical methods to be used for certain substances and residues thereof in live animals and animal products, Off. J. Eur. Commun. 221 (2002) 8–32.
[56] P.P. Eggertsen, J. Hansen, M.L. Andersen, J.F. Nielsen, R.K.J. Olsen, J. Palmfeldt, Simultaneous measurement of kynurenine metabolites and explorative metabolomics using liquid chromatography-mass spectrometry: a novel accurate method applied to serum and plasma samples from a large healthy cohort, J. Pharm. Biomed. Anal. 227 (2023) 115304, https://doi.org/10.1016/j.jpba.2023.115304.
[57] Y. Du, C. He, Y. An, Y. Huang, H. Zhang, W. Fu, M. Wang, Z. Shan, J. Xie, Y. Yang, B. Zhao, The role of short chain fatty acids in inflammation and body health, Int. J. Mol. Sci. 25 (2024) 7379, https://doi.org/10.3390/ijms25137379.
[58] J. He, P. Zhang, L. Shen, L. Niu, Y. Tan, L. Chen, Y. Zhao, L. Bai, X. Hao, X. Li, S. Zhang, L. Zhu, Short-chain fatty acids and their association with signalling pathways in inflammation, glucose and lipid metabolism, Int. J. Mol. Sci. 21 (2020) 6356, https://doi.org/10.3390/ijms21176356.